

Radislav A. Potyrailo · Gary M. Hieftje

## Use of the original silicone cladding of an optical fiber as a reagent-immobilization medium for intrinsic chemical sensors

Received: 16 October 1998 / Revised: 23 November 1998 / Accepted: 28 November 1998

**Abstract** It is demonstrated that extended-length sensors can be fabricated by the direct immobilization of suitable reagents into the original cladding of a plastic-clad silica (PCS) optical fiber. This cladding, a copolymer of vinyl-terminated poly(dimethylsiloxane) and poly(dimethylmethylhydrosiloxane), is an attractive immobilization matrix for a wide variety of reagents and opens up new avenues of sensor design. Unlike fibers with custom-drawn cladding, the new approach offers greater photo- and thermal stability and permits immobilization of several reagents in adjacent sections of a single fiber. Further, compared to room-temperature vulcanizable (RTV) silicone films used often in optical point sensors, the silicone cladding of a PCS optical fiber offers a number of advantages, including a dynamic fluorescence quenching constant for an immobilized fluorophore that is up to 3.4 times higher, tolerance to aggressive environments (e.g. highly alkaline solutions), lower rates of indicator leaching, high uniformity, and applicability to extended-length sensing. The homogeneity of the microenvironment of the fiber cladding, its resistance to aggressive alkaline solutions, and its ability to transport water vapor were probed by introducing a variety of reagents into the cladding, including a fluorescent ruthenium complex and acid-base and solvatochromic indicators. The new sensor-fabrication approach should find wide application, including detection of neutral species in gases and dissolved in water, and for spatial analyte mapping over extended, remote areas.

### Introduction

For acceptable performance of an indicator-based chemical sensor, a suitable analyte permeable host matrix for the

immobilized reagent must be found. An ideal such matrix should meet several criteria which include compatibility with a broad range of reagents, transparency at the analytical wavelengths, high and selective permeability to the analyte species of interest, excellent long-term stability under variable environmental conditions, ready availability, and simplicity of being incorporated into the sensor.

In optical sensors for neutral species, silicone is among the most often-used host matrices. Point sensors based on a variety of absorption and fluorescence reagents have been developed for detection of organic vapors [1, 2], chlorine [3], ammonia [4–8], simple amines [9], halothane [10] and sulfur dioxide [11]. One of the most common applications of such doped membranes is the detection of oxygen [10, 12–22] including *in vivo* measurements [23]. Advantages of this material over other polymers include relatively high analyte permeability, efficient dynamic quenching of immobilized fluorophores, and negligible luminescence at wavelengths above 300 nm [24, 25]. Readily available single-component room-temperature vulcanizable (RTV) silicone prepolymers allow the simple fabrication of sensing membranes with physically entrapped reagents, either by curing a dye-doped liquid prepolymer [1–8, 10, 11, 14, 21, 22] or by soaking the cured membrane in a dye cocktail [12, 13, 15–18]. The composition of the selected RTV prepolymer has a pronounced effect on sensor performance, especially those based on analyte-induced dynamic fluorescence quenching [17].

Reagent-doped silicone membranes are useful for the detection of species in gases and those dissolved in water; silicone is stable in pure water for years [26], absorbs only negligible quantities (< 0.1%) of water [27] and is not swollen by water appreciably [28]. In addition, hydrophobic silicone membranes are impermeable to ionic species, thereby enhancing sensor selectivity [7, 8].

Otherwise very attractive, common RTV matrices have several shortcomings which include poor solubility for polar indicators [7, 8, 14], inadequate resistance against highly alkaline solutions, which leads to rapid leaching of immobilized indicators [7] and problems involving at-

Dedicated to Professor Dr. Karl Cammann on the occasion of his 60th birthday

R. A. Potyrailo · G. M. Hieftje (✉)  
Department of Chemistry, Indiana University,  
Bloomington, IN 47405, USA

tachment to optical elements [24]. While the solubility of polar indicators in silicone can be improved by modifying them chemically [7, 8, 14, 29], it is hard to improve their resistance to an aggressive environment [30].

Realizing the advantages of silicone as a reagent-immobilization matrix, Blyler et al. [31, 32] doped special formulations of liquid silicones with analyte-sensitive reagents, applied these solutions onto the silica core of a multimode optical fiber to form the fiber cladding, and cured the cladding in-line during the fiber-drawing operation. By using this technology, Blyler et al. [31, 32] produced the first extended-length “intrinsic” sensors useful for spatially resolved analyte mapping. Because the analyte-sensitive reagent was distributed along the entire length of the fiber, analyte sensing could occur over extended regions, by means of evanescent-wave interaction with the reagent. Unfortunately, as admitted by the inventors [31–33], the technology suffered from several serious drawbacks. First, the photocuring chemistry involved the dissolved reagent and resulted in incomplete reversibility of the sensor. Second, the technology was complex, very expensive, and limited to those who have a fiber-optic drawing facility. Also, an organic reagent doped in the cladding was exposed to strong UV light (1 J/cm<sup>2</sup> over 300–400 nm spectral range) or high temperature (500 °C) required for the crosslinking of silicone during the fiber manufacture [31]; these conditions were likely to cause a partial degradation of a reagent.

The present paper describes an alternative and simpler approach for the fabrication of extended-length intrinsic sensors. The concept involves immobilization of reagents directly into the original (crosslinked) silicone cladding of a conventional low-cost plastic-clad silica (PCS) fiber [34]. In contrast to the method of Blyler et al. [31, 32], the new strategy does not involve photo- or temperature-induced degradation of an indicator, offers reversible sensor response, simplifies the fabrication process, lowers the construction cost of the sensing fiber, and permits immobilization of several reagents in adjacent sections of a single optical fiber for multianalyte determinations.

We demonstrate that the silicone cladding of a conventional PCS optical fiber offers a number of advantages over other common silicone materials used as host matrices for immobilization of indicators. These advantages are provided by both the composition and crosslink density of the silicone cladding. First, the cladding makes dynamic fluorescence quenching of an immobilized fluorophore more efficient than that provided by common RTV silicones. Remarkably, at high quencher concentrations, this efficiency is even higher than for the same fluorophores adsorbed on silica. Second, it shields an immobilized indicator from highly alkaline solutions and thus reduces indicator leaching or decomposition. Third, it is highly uniform, so it does not contribute significantly to light scattering in the optical fiber, and is thus useful for construction of extended-length sensors. Finally, it is already bound onto the fiber core, so there is no need for an additional matrix-fabrication step and the problem of attaching the membrane to an optical element is eliminated.

The PCS fiber cladding was evaluated as a reagent-immobilization matrix by incorporating into it a fluorescent ruthenium complex and also several acid-base indicators. As a result, the chemically modified fibers became sensitive to oxygen and ammonia, respectively. To evaluate the permeability of the fiber cladding to water vapor, a solvatochromic indicator was immobilized in the fiber cladding.

## Experimental

### Reagents and materials

Tris(1,10-phenanthroline) ruthenium(II) chloride (Ru(phen)<sub>3</sub>Cl<sub>2</sub>), sodium dodecyl sulfate (Na-DS), bromocresol green, phenol red, xylenol blue, and Nile red were obtained from Aldrich (Milwaukee, WI). All solutions were made with reagent-grade solvents that were obtained from commercial suppliers. Distilled deionized water was used throughout. The Ru(phen)<sub>3</sub>(DS)<sub>2</sub> complex was synthesized according to a literature method [14]. Multimode PCS 100/200N and PCS 200/300N (core-cladding diameters in micrometers, N-protective nylon jacket) optical fibers were obtained from Fiberguide Industries (Stirling, NJ). Dry nitrogen was supplied from boil-off of a local liquid-nitrogen storage facility. Compressed oxygen was obtained from Air Products and Chemicals (Allentown, PA). Wastewater samples were obtained from the Dillman Wastewater Treatment Plant (Bloomington, IN) at the initial and final points along the treatment process.

### Chemical modification of fiber cladding

The protocol for immobilizing indicators within the original fiber cladding involves five sequential steps: (1) removal of the protective nylon jacket from the fiber; (2) preparation of the indicator solution; (3) immobilization of the indicator into the fiber cladding by soaking the fiber in the indicator solution; (4) initial drying, rinsing with water followed by rinsing with ethanol until no indicator is visible in the rinsing solution; and (5) final drying of the chemically-modified optical fiber.

The protective nylon jacket was removed from the desired segment of a fiber by immersing it in boiling propylene glycol for 5 min [35]. The central portion of the exposed cladding was then coiled on a shaft 2.5 cm in diameter. Each indicator was immobilized in a separate fiber. For fluorescence measurements, a 1.8-m long coiled portion of a PCS 200/300N optical fiber was modified with a  $4 \times 10^{-6}$  M Ru(phen)<sub>3</sub>(DS)<sub>2</sub> solution in chloroform and another with a  $4 \times 10^{-6}$  M solution of Nile red in toluene. For absorption measurements, a 5 m coiled segment of a PCS 100/200N optical fiber was modified with a  $1 \times 10^{-4}$  M Nile red solution in toluene. Three 1.8 m long coiled sections of PCS 100/200N optical fiber were modified with  $1 \times 10^{-3}$  M bromocresol green, phenol red, and xylenol blue solutions in tetrahydrofuran (THF). The fibers were stored in air when not in use.

### Instrumentation

Spectra and response curves were obtained with an arrangement described in detail previously [36]. Briefly, light from a 65 W tungsten-halogen lamp was launched into the fiber by means of a microscope objective (numerical aperture (NA) of 0.4). The light transmitted through the fiber was dispersed by a 0.35-m grating monochromator and detected by a Hamamatsu R928 photomultiplier tube. Fluorescence measurements with optical fibers modified with Ru(phen)<sub>3</sub>(DS)<sub>2</sub> and Nile red were performed with an excitation interference filter (457 nm, bandwidth 6 nm). A 475 nm cutoff long-pass filter was placed at the output of the optical fiber to remove transmitted excitation light.

A solid-state fiber-optic sensor prototype was built for monitoring of ammonium-ion concentrations. In this sensor, light from

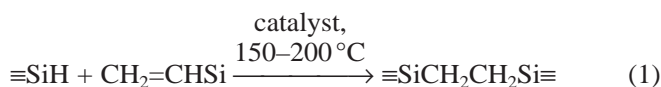
a green light-emitting diode (LED, 350 mcd,  $\lambda_{\max} = 568$  nm) was focused into the phenol-red-modified fiber by means of a microscope objective (NA = 0.4). The light transmitted through the fiber was sent to a silicon photodiode operating in the photovoltaic regime. The resulting output voltage was monitored as a function of analyte concentration. The sensor was calibrated and further used for monitoring of ammonium-ion concentrations in wastewater.

All gas-phase experiments were performed with dry nitrogen as a carrier gas. Required oxygen concentrations and levels of relative humidity were regulated by mass flow controllers, with the total flow maintained constant at 3 L/min. Relative humidity was monitored with a humidity monitor (Dickson, Addison, IL). Test samples of different ammonium-ion concentrations in water were made by adding portions of  $\text{NH}_4\text{Cl}$  or  $\text{NH}_4\text{OH}$  to a control solution of constant pH and ionic strength [37] (10 mM NaOH and 30 mM NaCl). All experiments were performed in laboratory conditions at atmospheric pressure.

## Results and discussion

### Nature of the silicone cladding of PCS optical fibers.

To better appreciate why the cladding of a PCS optical fiber is an attractive medium for immobilizing reagents useful for chemical sensing, it is worthwhile to examine the nature and properties of the cladding material. In its final form, the cladding is a clear silicone elastomer. However, it is initially obtained as a low-viscosity, two-component resin. This base resin and a crosslinker are vinyl-terminated poly(dimethylsiloxane) and poly(dimethylmethylhydrosiloxane), respectively (Fig. 1). Crosslinking is accomplished by mixing the base resin with the crosslinker in a 10:1 ratio and performing a rapid hydrosilylation reaction at elevated temperature [38] in the presence of a platinum catalyst [39]:



The liquid silicone mixture is applied to the silica core of the fiber and cured in-line during the fiber-drawing operation. Silicone elastomers produced in this way possess high crosslink density, toughness, tensile strength and dimensional stability because of the curing of the terminal vinyl groups of the base resin and the backbone structure

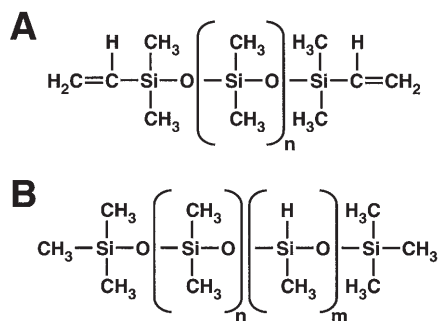


**Fig. 1** Structures of (A) base resin and (B) crosslinker components of silicone cladding in a PCS optical fiber

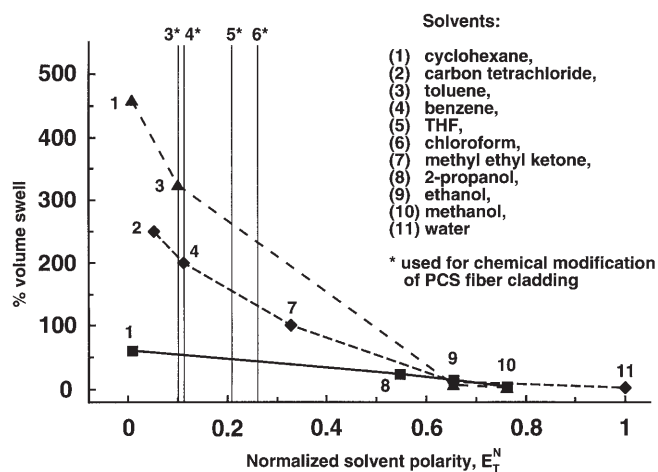


**Fig. 2** Swelling of silicone elastomers as a function of normalized solvent polarity: (triangles) lightly crosslinked poly(dimethylsiloxane) elastomer (data from Table 5 of ref. [41]); (diamonds) RTV silicone rubber (data from Table 96 of ref. [26]) (squares) silicone cladding of a PCS optical fiber (data from Table 1 of ref. [42]). For the direct comparison of swelling data of these silicones, employed solvents were arranged according to their normalized solvent polarity,  $E_T^N$ , relative to water ( $E_T^N = 1.000$ ) and tetramethylsilane ( $E_T^N = 0.000$ ) as described in ref. [43]

of the crosslinker. This crosslinked network is largely hydrophobic because of the non-polar poly(dimethylsiloxane) domains. However, limited regions of greater polarity are provided by the oxidized platinum catalyst present at part-per-million levels. Unlike silica-reinforced systems, this silicone elastomer maintains high optical clarity, which results in a homogeneous cladding material and therefore produces low Rayleigh-scattering losses [38].

The high crosslinking density in the cured elastomer limits its swelling in a variety of solvents, as indicated by the equilibrium swelling theory of Flory and Rehner [40]. According to this theory, the volume fraction  $v_2$  of polymer that is swollen is related to the number  $n$  of active chain segments in the network as

$$-\ln(1 - v_2) + v_2 + \chi v_2^2 = v_1 n [v_2^{1/3} - v_2/2] \quad (2)$$

where  $v_1$  is the molar volume of the solvent and  $\chi$  is the Flory-Huggins polymer-solvent interaction parameter. The number  $n$  of active chain segments in the network is directly proportional to the crosslink density [40]. Swelling of this cladding material in non-polar solvents is several times less than that of conventional silicone resins (Fig. 2). This minimal swelling affords the cladding a high level of resistance to most solvents [44].

### Immobilization solutions

Solvents for the preparation of indicator-immobilization solutions were selected to satisfy three criteria, including the ability (i) to dissolve a particular indicator, (ii) to swell the silicone cladding, enabling the indicator to diffuse to regions near the core-cladding interface, and (iii) not to dissolve the cladding.

Since the indicators are immobilized by physical entrapment in the polymer matrix, both the magnitude of swelling of the cladding and the size of the indicator molecules are important for success. More than 30 indicators of different sorts (polycyclic aromatic hydrocarbons, rhodamines, coumarins, cyanides, sulfonaphthaleins, azo-dyes, porphyrins, and others) have been successfully immobilized into the silicone cladding of PCS fibers by utilizing a variety of non-polar solvents.

Suitable solvents for the classes of indicators investigated here have been found to be benzene, chloroform, THF, and toluene. They provided a 45–55% swelling of the cladding (cf. Fig. 2), sufficient for the immobilization of indicators. These solvents have normalized solvent polarities  $E_T^N$  ranging from 0.099 to 0.259 relative to water ( $E_T^N = 1.000$ ) and tetramethylsilane ( $E_T^N = 0.000$ ) [43]. Although the extent of silicone swelling increases with lower solvent polarity [28], the solvents were selected not to be too non-polar in order to dissolve a wide range of indicators.

The molecular weight of the immobilized indicators spanned almost an order of magnitude from 140 (nitrophenol) to 1200 (Ru(phen)<sub>3</sub>(DS)<sub>2</sub> complex). It is possible that this range could be broader; however, it encompasses most fluorescence and absorption indicators.

The concentration of each indicator in its immobilization solution was optimized individually for a particular application. For example, a fluorophore should not be added at levels where self-quenching becomes significant. With a properly selected solvent, the immobilized indicator did not crystallize in the fiber cladding, even at relatively high doping levels (from  $1 \times 10^{-3}$  M immobilization solutions) after almost two years of storage, as verified by optical microscopy.

#### Real-time monitoring of indicator-immobilization process

During early trials, it was found useful to monitor the rate at which a chosen indicator was incorporated into the cladding host. Such monitoring can reveal accumulation of indicator molecules at the interface between the polar silica core and the non-polar silicone cladding, and can aid in selecting an optimal duration for soaking the fiber in an immobilization solution and for drying it after the indicator is immobilized. The monitoring was ordinarily accomplished by measuring the evanescent-wave transmittance of the modified-cladding fiber. This measurement has its own boundary conditions. In a PCS optical fiber, the refractive index of the fiber core is  $n_{co} = 1.46$ , greater than the refractive index of the fiber cladding,  $n_{cl} = 1.41$ . The light launched into the fiber propagates in the core within a range of angles of incidence  $\phi$  defined with respect to the normal to the core/cladding interface. This range is given by

$$\phi_c \leq \phi \leq 90^\circ \quad (3)$$

where  $\phi_c$  is the critical angle,  $\phi_c = \sin^{-1}(n_{cl}/n_{co})$ .

When a PCS fiber is soaked in an immobilization solution, the refractive index of the cladding approaches that

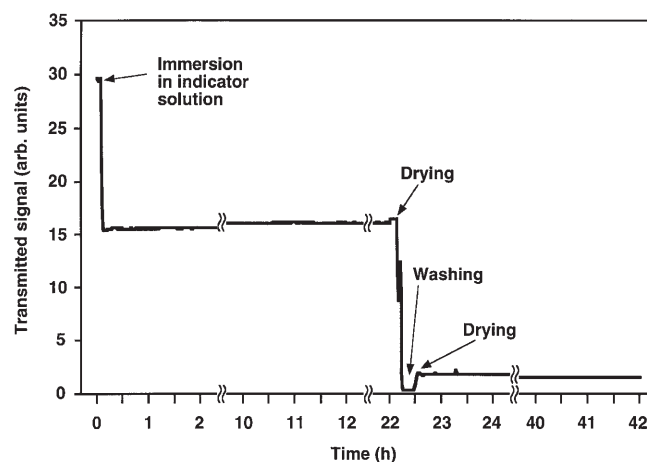


**Fig. 3** Optical-fiber transmittance change during the immobilization of phenol red into the silicone cladding of a PCS optical fiber. The probe wavelength (390 nm) is at the absorption maximum of phenol red in THF, the solvent used for immobilization

of the bulk solution,  $n_{sol}$ , due to the swelling of the cladding in the solvent. To maintain the condition given by Eq. 3, the indicator-immobilization process should be monitored only when  $n_{sol} < n_{co}$ ; otherwise, the light launched into the fiber escapes through the swollen cladding into the bulk immobilization solution.

How a typical fiber transmittance changes with time during the immobilization steps is shown in Fig. 3. In this experiment, a 9-m long PCS fiber was soaked in a  $1.4 \times 10^{-3}$  M phenol red solution in THF ( $n_{THF} = 1.40$ ). The probe wavelength was 390 nm, which corresponded to the absorption maximum of the indicator solution. Diffusion of the dissolved indicator into the swollen fiber cladding caused a rapid drop in fiber transmittance, caused in turn by attenuation of the evanescent-wave amplitude by the absorbing indicator. This signal stabilized within several minutes of immersion of the fiber into the immobilization solution and remained virtually constant during the next 22 h when the fiber was kept in solution. This stability suggested that there was no accumulation of indicator molecules at the core/cladding interface. In all subsequent experiments, the immobilization step was limited to about 15–30 min. The initial 15 min drying after indicator immobilization was followed by rinsing the fiber and its final drying for several hours.

Of course, the first step in the immobilization protocol can be eliminated if PCS fibers originally drawn for fiber-bundle fabrication and thus with no protective jacket are employed. The use of a jacket-free PCS fiber is especially advantageous for construction of a “distributed” sensor with a continuous sensing fiber that is tens or hundreds of meters long.

#### Fiber cladding doped with a dynamically-quenched fluorescence indicator

The degree of homogeneity of an immobilization matrix is one of the most important considerations in designing a

sensor based on dynamic fluorescence quenching of an immobilized fluorophore. Even in situations where quenching is known to be purely dynamic (not static), Stern-Volmer calibration plots exhibit a downward curvature if the immobilization matrix offers a heterogeneous microenvironment to the indicator [13, 25, 45, 46].

As a result, a two-site quenching model is commonly employed to analyze Stern-Volmer quenching curves for dye-doped silicone membranes [13]. In this model, the immobilized indicator exists in two different environments which yield two different forms. One form involves homogeneously distributed molecules, while the other involves aggregates. Upon exposure to quenching species Q, both indicator forms are quenchable but with different quenching constants  $K_{SV1}$  and  $K_{SV2}$  and weighting factors  $f_1$  and  $f_2$ . The basic equation for the model is given by [13]

$$I_0/I = \frac{1}{f_1/(1 + K_{SV1}[Q]) + f_2/(1 + K_{SV2}[Q])} \quad (4)$$

Larger ratios  $K_{SV1}/K_{SV2}$  and  $f_1/f_2$  signify a more homogeneous microenvironment for an immobilized fluorophore.

The microheterogeneity of the cladding material was evaluated by incorporating into it an oxygen-sensitive Ru complex. The highly fluorescent Ru(phen)<sub>3</sub> complex was selected for this study because it was extensively used in the past for the fabrication of extrinsic sensors for oxygen [14, 19, 47–50]. Its photophysics and photochemistry as well as potential interferences have also been investigated in great detail [13, 14, 51]. The solubility of the selected Ru complex in non-polar solvents was increased by replacing the inorganic chloride ions by organic DS ions [14]. This straightforward molecular modification does not affect the quenching properties of the Ru(phen)<sub>3</sub> com-

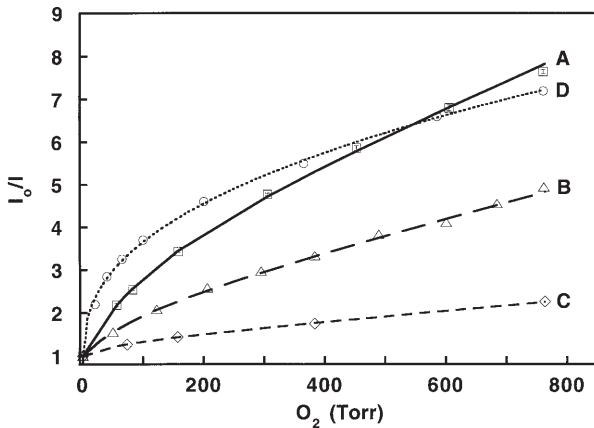


**Fig. 4** Non-linearity of the Stern-Volmer calibration plots for oxygen sensors based on a Ru(phen)<sub>3</sub> complex immobilized in different matrices: A, silicone cladding of a PCS optical fiber; B, GE RTV 118 silicone film (experimental points taken from Fig. 4B of ref. [13]); C, single-component RTV acetic acid-releasing silicone film (experimental points taken from Fig. 3 of ref. [14]); D, hydrophilic fumed silica (experimental points taken from Fig. 8B of ref. [46]). For sensor A, the 95% confidence intervals are given for 5 replicate measurements. Fluorescence emission signal was collected at 610 nm with an excitation wavelength of 457 nm

plex because the spectral and photophysical properties of the indicator are determined almost exclusively by the chromophore [14].

The fluorescence-quenching data were fitted to Eq. 4 in order to compare the ratios  $K_{SV1}/K_{SV2}$  and  $f_1/f_2$  for the new sensor to those for other oxygen sensors based on the same indicator immobilized in films made from single-component RTV silicones [13, 14]. So far, these materials have provided the largest oxygen-quenching constants for immobilized Ru(phen)<sub>3</sub> and for other fluorophores in point sensors [13, 14, 16, 25].

Figure 4 compares the Stern-Volmer calibration curve for the new sensor (curve A) with those for sensors reported by Demas and co-workers [13] (curve B) and Klimant and Wolfbeis [14] (curve C). These sensors [13, 14] were selected for comparison because both utilize the same Ru complex as employed here but immobilized in RTV silicone. Figure 4 illustrates that the new sensor has the greatest sensitivity for oxygen determinations at both low and high concentrations. At 760 Torr, dynamic fluorescence quenching of the immobilized Ru(phen)<sub>3</sub> complex by molecular oxygen is between 1.5 and 3.4 times more efficient in the fiber cladding than in home-cast silicone films. The lowest partial pressure of oxygen used in these experiments was 56 Torr. The detection limit for the sensor (at a S/N = 3) calculated from the slope of the calibration curve over the lowest range of partial pressures was 0.12 Torr (at an integration time of 10 s). The relative standard deviation (RSD) for five repeated measurements over the range of measured partial pressures of oxygen was  $\leq 0.5\%$ . Other investigations [13, 14] did not cite values for precision and detection limit.

The fitting parameters of the model described by Eq. 4 for the three Ru(phen)<sub>3</sub> sensors are compiled in Table 1. The ratio  $K_{SV1}/K_{SV2}$  is 20 to 150% larger and the ratio  $f_1/f_2$  is 17.5 to 2.8 times larger for the new sensor than for the other sensors. These data suggest that the homogeneously distributed form of the dye contributes more to the total fluorescence quenching in the silicone fiber-cladding material than it does in home-cast silicone films.

The greater homogeneity of the fluorophore distribution in the cladding material is most likely the result of its material properties. The silicone in the cladding is more highly crosslinked than it is in conventional RTV silicones used previously in oxygen sensors [13, 14, 16]. This high network density leads to reduced aggregation of

**Table 1** Two-site model oxygen-quenching fitting parameters for Ru(phen)<sub>3</sub> sensors<sup>a</sup>

Sensor	$K_{SV1}$ Torr <sup>-1</sup>	$K_{SV2}$ Torr <sup>-1</sup>	$K_{SV1}/K_{SV2}$	$f_1$	$f_2$	$f_1/f_2$	$\chi^2$
Sensor A	0.02956	0.000905	32.7	0.84	0.16	5.25	0.0071
Sensor B <sup>b</sup>	0.0197	0.0015	13.1	0.65	0.35	1.86	0.025
Sensor C <sup>c</sup>	0.0275	0.0010	27.5	0.23	0.77	0.30	

<sup>a</sup> see Eq. 4 and Fig. 4

<sup>b</sup> ref. [13]

<sup>c</sup> ref. [14]

immobilized indicator molecules. In a chemical sensor that employs dynamically quenched fluorescence, reduced reagent aggregation results in more effective fluorescence quenching (cf. Table 1). In addition, the poly(dimethylsiloxane)-rich cladding material provides excellent solubility for the non-polar Ru(phen)<sub>3</sub>(DS)<sub>2</sub> complex [17]. Overall, the Ru complex immobilized in a silicone cladding fits perfectly the domain model proposed by Demas and co-workers [17] with a dominant hydrophobic domain whose major constituent is poly(dimethylsiloxane).

It is useful also to compare the quenching curve for the Ru complex when it is immobilized in silicone (Figure 4, curve A) to that when it is adsorbed on hydrophilic fumed silica [46] (Fig. 4, curve D). Oxygen adsorption on fumed silica obeys the Freundlich model for gas-solid adsorption [52], which describes the relation between the fractional surface coverage  $\theta$  of the adsorbate and the equilibrium gas-phase pressure  $P$ :  $\theta = a P^{1/b}$ , where  $a$  and  $b$  are constants. The diffusional quenching of a silica-bound fluorophore by adsorbed oxygen can be described by a two-parameter Stern-Volmer quenching expression [46]:

$$I_0/I = 1 + K_{SV}[Q]_{adsM} a P^{1/b} \quad (5)$$

where  $[Q]_{adsM}$  is the maximum surface concentration of the quencher. The best fit to the quenching data of curve D [46] indicated that, as expected, the quenching constant term ( $K_{SV}[Q]_{adsM} a = 0.98 \text{ cm}^{-1} \text{ Hg}$ ) was greater than that for the silicone-based sensors (see Table 1). However, as illustrated in Fig. 4, the oxygen-quenching curve for the silica-adsorbed Ru complex deviates substantially from Stern-Volmer behavior. At 760 Torr oxygen the quenching efficiency of the new sensor (curve A) is roughly 10% higher than that of sensor D.

The dynamic response of the developed oxygen sensor was evaluated in a series of breathing experiments. The experimenter inhaled and exhaled through a small cell via a 15 cm long, 0.6 cm diameter plastic tube. For the doped PCS 200/300 optical fiber the response time was anticipated to be about 0.1–0.3 s, on the basis of literature diffusion coefficients of oxygen in different types of unfilled silicones [53, 54], which range from  $1.6 \times 10^{-5}$  to  $3.6 \times 10^{-5} \text{ cm}^2/\text{s}$ . Although the sensor responded fast enough to faithfully follow oxygen concentrations during breathing, the response time was about 1 s, due to the time required to change the gas environment in the sample cell and the finite gas-flow resistance of the tube. If necessary, the response time of the sensor should be able to be reduced to the range of 0.1–0.3 s by simple improvements in the gas-introduction arrangement and by miniaturization of the cell. The response time could be shortened also by utilizing an optical fiber with a thinner silicone cladding; the response time drops as the square of cladding thickness [55]. For example, instead of the PCS 200/300 fiber with a 50  $\mu\text{m}$  thick cladding used in the present studies, a PCS 210/230 fiber could be utilized with a cladding only 7.5  $\mu\text{m}$  thick. The use of the thinner cladding should result in a 45 times faster (3–7 ms) dynamic response.

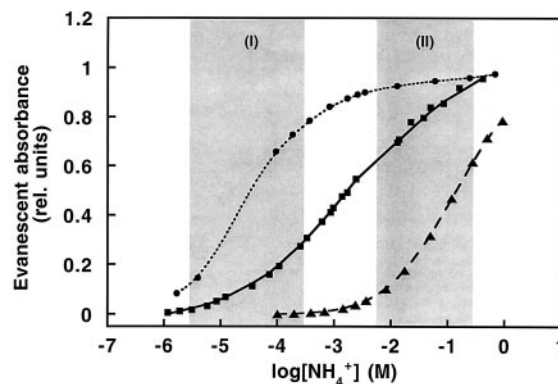


**Fig. 5** Working curves for indicator-doped fibers measured at the peak of the indicator absorption band. Immobilized indicators and probe wavelengths: (circles) bromocresol green, 615 nm; (squares) phenol red, 565 nm; (triangles) xylenol blue, 595 nm. Concentration ranges of (I) environmental and (II) industrial interest

#### Fiber cladding doped with acid-base indicators

The resistance of the reagent-doped silicone cladding to aggressive alkaline solutions is important in sensors intended for high ammonia concentrations. Previous attempts to develop a sensor useful for such determinations, without sample dilution, suffered from leaching of the immobilized indicator [7].

Different fibers were doped with chosen sulfonaphthalein indicators with different acid-dissociation constants. Calibration curves for the modified fibers (Fig. 5) were obtained at the absorption peak of the base form of each respective indicator. A key feature of the new sensors is their ability to withstand continuous exposure to a highly alkaline medium and to detect high base concentrations such as those found in industrial production of ammonia, ammonium nitrate and ammonium sulfate [56] where the concentration range of ammonium ions is from  $5.6 \times 10^{-3}$  to  $2.8 \times 10^{-1} \text{ M}$ . The RSD for three replicate measurements of ammonium ions in this concentration range with the phenol red solid-state sensor during a month of experiments was less than 1%. The total exposure time to concentrated ammonium-ion solutions in these measurements was 4 h. Long-term tests of the phenol-red sensor to aqueous solutions of 14 M  $\text{NH}_4\text{OH}$  and 10 M NaOH revealed no observable washout of the immobilized indicator over a period of several months [34]. This stability can be attributed to the highly crosslinked fiber cladding material [26], which makes the cladding extremely resistant to degradation by alkaline solutions.

The new ammonia sensors exhibit a usefully broad dynamic range. As shown in Fig. 5, the bromocresol-green and phenol-red sensors can be used for determination of ammonium ions in the concentration range of environmental interest [57] ( $2.8 \times 10^{-6}$  –  $2.8 \times 10^{-4} \text{ M}$ ) in drinking, river, and wastewater. The detection limit for the bromocresol green sensor was calculated to be 20 nM ( $S/N = 3$ , integration time 1 s). The dynamic range of the phenol-red sensor was about six orders of magnitude,

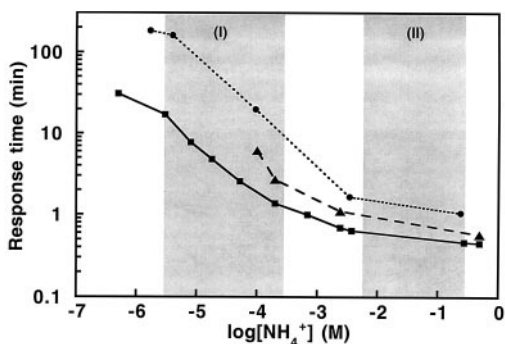


**Fig. 6** Response time of the ammonium-ion sensors as a function of analyte concentration. Immobilized indicators: (*circles*) bromocresol green; (*squares*) phenol red; (*triangles*) xylenol blue. Concentration ranges of (*I*) environmental and (*II*) industrial interest

making it possible to monitor both ranges of interest, environmental and industrial (cf. Fig. 5). The phenol-red sensor demonstrated a 24-nM detection limit ( $S/N = 3$ , integration time 3 s).

In contrast to the performance of a distributed fiber-optic sensor for ammonia gas based on a PCS fiber drawn with an indicator-doped cladding [32], the response of the new sensors is completely reversible [58]. The incomplete reversibility of the sensor of Blyler et al. [32] was a result of the photocuring chemistry which interfered with the dissolved reagent. In the sensors reported here, there is no chemical interaction between the immobilized dye and the silicone network, as indicated by the similarity of absorption spectra of the dissolved and entrapped dyes [58].

The dynamic response of the new sensors was studied as a function of the external concentration of ammonium ions (Fig. 6). The response time (measured at 90% of the maximum signal change) was approximately inversely proportional to the analyte concentration. Although the bromocresol-green sensor had the highest sensitivity at low analyte concentrations, its response time was unacceptably long for many practical applications. In contrast, the phenol-red sensor had the fastest response, ranging from 1 to 17 min over the concentration range of environmental interest and about 0.5 min over the concentration range of industrial interest.

Ammonia in local wastewater samples was determined to establish the analytical utility of the sensor in a working environment. For these experiments, the phenol-red solid-state sensor was used. The pH of the wastewater samples was adjusted to that of the control solution and ammonia concentrations were determined by standard additions. The reference values, obtained with an ammonia-selective electrode, were provided by the wastewater-treatment plant: concentration of ammonia nitrogen was 8.8 and 11.8 ppm in influent samples and 0.02 and 0.03 ppm in effluent samples. Measurements with the fiber-optic sensor yielded  $12.9 \pm 0.3$  and  $14.3 \pm 0.4$  ppm in influent samples and  $0.015 \pm 0.006$  and  $0.032 \pm 0.008$  ppm in effluent samples (mean  $\pm$  SD;  $n = 3$ ). An

agreement of  $R = 0.99$  between the fiber-optic sensor and the reference method was found.

#### Fiber cladding doped with a solvatochromic indicator

Liquid water has a very low solubility in silicone. On the other hand, silicones are highly permeable to water vapor [26, 53]. This high permeability might alter the non-polar environment within the silicone cladding and affect the behavior of a variety of immobilized indicators. The influence of water vapor on the properties of the silicone cladding was investigated by spectroscopic means. For this purpose, the cladding was doped with Nile red, a common solvatochromic dye.

Evanescent-wave absorption and fluorescence spectra of immobilized Nile red were investigated when the modified fibers were exposed to dry and moist nitrogen of 85% relative humidity (Fig. 7). The absorbance of the modified fiber was lowered upon addition of water vapor to the test chamber. The absence of a noticeable shift in the 522-nm absorption peak for the immobilized Nile red (Fig. 7A) was similar to the behavior of the free dye subjected to hydrogen-bonding solvents [59]. The fluorescence spectra (Fig. 7B) were affected slightly by the humidity difference. These data suggest that reagents to be used for sensing in this type of device should be selected to be affected as little as possible by water vapor or that the sensor be used in applications where the concentration of water vapor is unlikely to change greatly; alternatively, it might be possible to correct the sensor response for the presence of water vapor if an independent means of humidity or moisture measurement is available.

The sorption and desorption of water vapor in the silicone fiber cladding was completely reversible, as verified by monitoring of the hypochromic effect at 522 nm. A typical dynamic response of the Nile-red modified fiber is

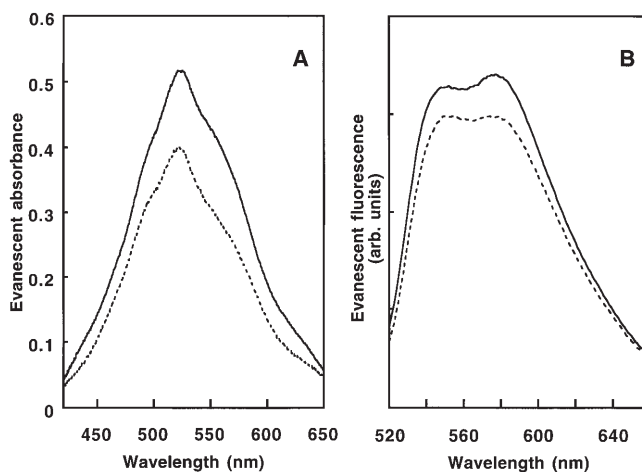


**Fig. 7** Evanescent-wave (A) absorption and (B) fluorescence spectra of the immobilized Nile red in (*solid line*) dry nitrogen and (*dashed line*) nitrogen at 85% relative humidity. Fluorescence-excitation wavelength, 457 nm

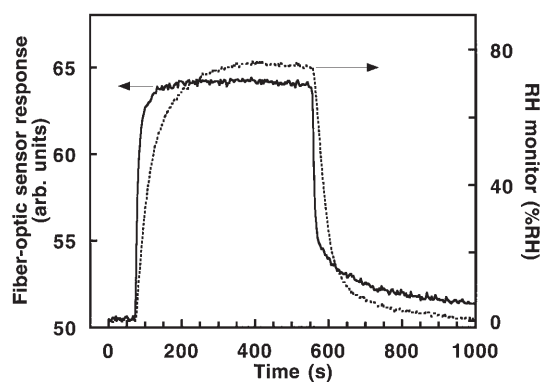


**Fig. 8** Dynamic response to change in relative humidity; (solid line) PCS optical fiber modified with Nile Red and (dashed line) a commercial humidity monitor. Fiber transmittance was monitored at 522 nm

compared with that of a humidity monitor in Fig. 8. The response time of the fiber-optic sensor was less than 1 min, while the recovery time was an order of magnitude longer, presumably due to the slow vapor desorption. These data illustrate the feasibility of using dye-doped silicone-cladding sensors for continuous humidity monitoring over extended areas, possibly for early detection of moisture-induced corrosion in structural components in civil, aerospace, and electrical engineering.

## Conclusions

Use of the silicone cladding of a PCS optical fiber as a reagent-immobilization medium results in a dramatic improvement in sensor performance compared to point sensors that utilize films made from conventional RTV silicone resins. This improvement is provided by both the composition and high crosslink density of the silicone cladding. For example, the Ru(phen)<sub>3</sub> cation exhibits the highest oxygen-quenching constant reported when immobilized in a silicone elastomer. The cladding also provides protection for an immobilized indicator in highly alkaline solutions and thus prevents indicator leaching.

The new approach to fabricating optical-fiber transducers maintains the structural integrity of the fiber and does not add to light-scattering losses since the original cladding is not replaced. In contrast, re-clad optical fibers often suffer from lack of cladding uniformity, scattering losses, and lack of mechanical flexibility. Although only 2–9 m long segments were used in the present study, chemically-modified fibers could be fabricated over a length limited only by the original fiber spool and could then be cut into segments of desired length. In the future, this sensor-fabrication concept should allow detection of a wide range of species in gaseous and aqueous phase and with the capability for spatial analyte mapping over extended, remote areas.

**Acknowledgements** Our thanks go to F.V. Bright (SUNY, Buffalo, NY), I. Camlibel, Fiberguide Industries (Stirling, NJ), J.N. Demas (University of Virginia, Charlottesville, VA), and J.H. Mac Millan (United Chemical Technologies, Inc.) for stimulating discussions and to M.A. Gudeman and C. A. Abbott (Dillman Wastewater Treatment Plant, Bloomington, IN) for providing wastewater samples and reference data. This work was supported in part by the National Institutes of Health through grant GM 53560. R.A.P. gratefully acknowledges the support of Boehringer Mannheim Corp. (USA) for a Summer Research Fellowship and the College of Arts and Sciences, Indiana University for a McCormick Science Grant.

## References

- Barnard SM, Walt DR (1991) *Environ Sci Technol* 25: 1301–1304
- Angel SM, Anderson BL, Langry K (1991) *Proc SPIE-Int Soc Opt Eng* 1587: 86–95
- Brook TE, Narayanaswamy R (1997) *Sens Actuators B* 38–39: 195–201
- Reichert J, Sellien W, Ache HJ (1991) *Fresenius J Anal Chem* 339: 467
- Gaughlitz G, Kraus G (1993) *Fresenius J Anal Chem* 346: 572–576
- Potyrailo RA, Golubkov SP, Borsuk PS, Talanchuk PM, Novoselov EF (1994) *Analyst* 119: 443–448
- Werner T, Klimant I, Wolfbeis OS (1995) *Analyst* 120: 1627–1631
- Trinkel M, Trettnak W, Reininger F, Benes R, O'Leary P, Wolfbeis OS (1996) *Anal Chim Acta* 320: 235–243
- Borsuk PS, Golubkov SP, Potyrailo RA (1990) *Soviet Patent* 1775647
- Wolfbeis OS, Posch HE, Kroneis HW (1985) *Anal Chem* 57: 2556–2561
- Wolfbeis OS, Sharma A (1988) *Anal Chim Acta* 208: 53–58
- Bacon JR, Demas JN (1987) *Anal Chem* 59: 2780–2785
- Carraway ER, Demas JN, DeGraff BA, Bacon JR (1991) *Anal Chem* 63: 337–342
- Klimant I, Wolfbeis OS (1995) *Anal Chem* 67: 3160–3166
- Berndt KW, Lakowicz JR (1992) *Anal Biochem* 201: 319–325
- Sacksteder L, Demas JN, DeGraff BA (1993) *Anal Chem* 65: 3480–3483
- Xu W, McDonough RC, Langsdorf B, Demas JN, DeGraff BA (1994) *Anal Chem* 66: 4133–4141
- Xu W, Kneas KA, Demas JN, DeGraff BA (1996) *Anal Chem* 68: 2605–2609
- Hartmann P, Ziegler W (1996) *Anal Chem* 68: 4512–4514
- Chuang H, Arnold MA (1997) *Anal Chem* 69: 1899–1903
- Mills A, Lepre A, Theobald BRC, Slade E, Murrer BA (1997) *Anal Chem* 69: 2842–2847
- Hobbs SE, Potyrailo RA, Hieftje GM (1997) *Anal Chem* 69: 3375–3379
- Miller WW, Yafuso M, Yan CF, Hui HK, Arick S (1987) *Clin Chem* 33: 1538–1542
- Wolfbeis OS (ed) (1991) *Fiber Optic Chemical Sensors and Biosensors*. CRC Press, Boca Raton, FL
- Draxler S, Lippitsch ME, Klimant I, Kraus H, Wolfbeis OS (1995) *J Phys Chem* 99: 3162–3167
- Noll W (1968) *Chemistry and Technology of Silicones*. Academic Press, New York, NY
- Cash CG (1970) In: Bruins PF (ed) *Silicone Technology*. Interscience Publishers, New York, NY, pp 47–50
- Flory PJ (1953) *Principles of Polymer Chemistry*. Cornell University Press, New York, NY
- Marsoner H, Kroneis H, Wolfbeis O (1987) *US Patent* 4, 657, 736
- Hui HK, Divers GA III, Soikowski C (1993) *US Patent* 5, 182, 353
- Blyler LL, Jr, Cohen LG, Lieberman RA, MacChesney JB (1989) *US Patent* 4, 834, 496

32. Blyler LL, Jr, Lieberman RA, Cohen LG, Ferrara JA, MacChesney JB (1989) *Polymer Eng Sci* 29: 1215–1218
33. Lieberman RA (1993) *Sens Actuators B* 11: 43–55
34. Potyrailo RA, Hieftje GM (1995) Pittsburgh Conference Paper 1022
35. DeGrandpre MD, Burgess LW (1988) *Anal Chem* 60: 2582–2586
36. Potyrailo RA, Ruddy VP, Hieftje GM (1996) *Appl Opt* 35: 4102–4111
37. Rhines TD, Arnold MA (1988) *Anal Chem* 60: 76–81
38. Blyler LL, Jr, Eichenbaum BR, Schonhorn H (1979) In: Miller SE, Chynoweth AG (eds) *Optical Fiber Telecommunications*. Academic Press, New York, NY; pp 299–341
39. Larson R, Smith C (eds) (1991) *Silicon Compounds: Register and Review*. Huls America, Inc., Piscataway, NJ
40. Sperling LH (1986) *Introduction To Physical Polymer Science*. Wiley-Interscience, New York, NY
41. Baney RH, Voigt CE, Mentle JW (1977) In: Harris FW, Seymour RB (eds) *Structure-Solubility Relationships in Polymers*. Academic Press, New York, NY; pp 225–232
42. Blair DS, Burgess LW, Brodsky AM (1995) *Appl Spectrosc* 49: 1636–1645
43. Reichart C (1994) *Chem Rev* 94: 2319–2358
44. Guillet J (1985) *Polymer Photophysics and Photochemistry*. Cambridge University Press, Cambridge, UK
45. Demas JN, DeGraff BA (1993) *Sens Actuators B* 11: 35–41
46. Carraway ER, Demas JN, DeGraff BA (1991) *Langmuir* 7: 2991–2998
47. Carraway ER, Demas JN, DeGraff BA (1991) *Anal Chem* 63: 332–336
48. Rosenzweig Z, Kopelman R (1995) *Anal Chem* 67: 2650–2654
49. He H, Fraatz RJ, Leiner MJP, Rehn MM, Tusa JK (1995) *Sens Actuators B* 29: 246–250
50. Gouin JF, Baros F, Birot D, Andre JC (1997) *Sens Actuators B* 38–39: 401–406
51. Rosenzweig Z, Kopelman R (1996) *Anal Chem* 68: 1408–1413
52. Freundlich H (1926) *Colloid and Capillary Chemistry*. Methuen, London
53. Robb WL (1968) In: Levine SN (ed) *Materials in Biomedical Engineering*. The New York Academy of Sciences, New York, Vol. 146, Art. 1; pp 119–137
54. Cox ME, Dunn B (1986) *J Polymer Sci: Part A: Polymer Chemistry* 24: 621–636
55. Crank J, Park GS (eds) (1968) *Diffusion in Polymers*. Academic Press, London
56. Bolto BA, Pawlowski L (1987) *Wastewater Treatment by Ion-Exchange*. E. & F. N. Spon, London
57. Tebbutt THY (1992) *Principles of Water Quality Control*. Pergamon Press, Oxford
58. Potyrailo RA, Hieftje GM (1995) *FACSS XXII Annual Meeting Paper* 335
59. Deye JF, Berger TA, Anderson AG (1990) *Anal Chem* 62: 615–622